Inorg. Chem. **2006**, *45*, 10815–10824

Radical Salts of Bis(ethylenediseleno)tetrathiafulvalene with Paramagnetic Tris(oxalato)metalate Anions

Eugenio Coronado,[†] Simona Curreli,[†] Carlos Giménez-Saiz,*[,†] Carlos J. Gómez-García,*[,†] and Antonio Alberola[‡]

Instituto de Ciencia Molecular, Edificio de Institutos de Paterna, Universidad de Valencia, P.O. Box 22085, 46071 Valencia, Spain, and Department of Chemistry, The University of Cambridge, Lensfield Road, Cambridge CB2 1EW, U.K.

Received August 8, 2006

The synthesis, crystal structure, and physical characterization of five new radical salts formed by the organic donor bis(ethylenediseleno)tetrathiafulvalene (BEST) and the paramagnetic tris(oxalato)metalate anions $[M(C_2O_4)_3]^{3-}$ (M = Fe^{III} and Cr^{III}) are reported. The salts isolated are $(BEST)_4[M(C_2O_4)_3]\cdot PhCOOH\cdot H_2O$ with M^{III} = Cr (**1**) or Fe (**2**) (crystal data: **1**, triclinic, space group $P\bar{1}$ with a = 14.0999(4) Å, b = 15.3464(4) Å, c = 19.5000(4) Å, α = 76.711(5)°, β = 71.688(5)°, γ = 88.545(5)°, V = 3893.5(2) Å^3, and Z = 2; **2**, triclinic, space group $P\bar{1}$ with a = 14.0326(3) Å, b = 15.1981(4) Å, c = 19.4106(4) Å, α = 76.739(5)°, β = 71.938(5)°, γ = 88.845(5)°, V = 3824.9(2) Å^3, and Z = 2), $(BEST)_4[M(C_2O_4)_3]\cdot 1.5H_2O$ with M^{III} = Cr (**3**) or Fe (**4**) (crystal data: **3**, monoclinic, space group $C2/m$ with a = 33.7480(10) Å, b = 12.3151(7) Å, c = 8.8218(5) Å, β = 99.674(5)°, V = 3614.3(3) Å^3, and Z = 2; **4**, monoclinic, space group $C2/m$ with a = 33.659(6) Å, b = 12.248(2) Å, c = 8.759(2) Å, β = 99.74(3)°, V = 3558.9(12) Å^3, and Z = 2), and $(BEST)_9[Fe(C_2O_4)_3]_2\cdot 7H_2O$ (**5**) (crystal data: triclinic, space group $P\bar{1}$ with a = 12.6993(3) Å, b = 18.7564(4) Å, c = 18.7675(4) Å, α = 75.649(5)°, β = 107.178(5)°, γ = 79.527(5)°, V = 3977.5(3) Å^3, and Z = 1). The structures of all these salts consist of alternating layers of the organic donors and tris(oxalato)metalate anions. In **1** and **2** the anionic layers contain also benzoic acid molecules H-bonded to the terminal oxygen atoms of the anions. In all salts the organic layers adopt β-type packings. Along the parallel stacks the donors form dimers in **3** and **4**, trimers in **5**, and tetramers in **1** and **2**. All the compounds are paramagnetic semiconductors with high room-temperature conductivities and magnetic susceptibilities dominated by the Fe- or Cr-containing anions.

Introduction

During the past few years the design and synthesis of new molecular materials with unusual combination of physical properties as, for example, compounds coupling magnetic and conducting sublattices has become one of the most appealing challenges in the chemistry of materials.[1] This novel class of multifunctional materials should provide a unique opportunity to study the physics arising from the competition and interplay of these properties. An attractive approach for the design of these materials is to make two-network solids formed by alternating layers of partially oxidized organic π-electron donor molecules of the tetrathiafulvalene (TTF) family, which support electronic conduction, and layers of charge-compensating magnetic anions. The charge, shape, and volume of the counteranions also play an important role as they can force the donor molecules to pack in different arrangements and so influence the electrical properties.[2]

This approach has already led to a rich harvest of hybrid molecular materials combining magnetism with conductivity, such as paramagnetic[3] or antiferromagnetic[4] superconductors and ferromagnetic conductors.[5] Most of these interesting results have been obtained using tris(oxalato)metalate complexes as counteranions in the preparation of conducting

* To whom correspondence should be addressed. E-mail: carlos.gimenez@uv.es (C.G.-S.), carlos.gomez@uv.es (C.J.G.-G.).
[†] Universidad de Valencia.
[‡] The University of Cambridge.

(1) (a) Coronado, E.; Day, P. *Chem. Rev.* **2004**, *104*, 5419. (b) Enoki, T.; Miyazaki, A. *Chem. Rev.* **2004**, *104*, 5449. (c) Kobayashi, H.; Cui, H. B.; Kobayashi, A. *Chem. Rev.* **2004**, *104*, 5265.

(2) Coronado, E.; Giménez-Saiz, C.; Gómez-García, C. J. *Coord. Chem. Rev.* **2005**, *249*, 1776.

10.1021/ic061494p CCC: $33.50
Published on Web 11/18/2006

radical cation salts. The series of molecular materials having the general formula $(ET)_4[(H_3O)M(C_2O_4)_3]\cdot G$ (where ET = bis(ethylenedithio)tetrathiafulvalene, M^{III} = Fe, Cr, Co, Al, and Ga, and G = PhCN, $PhNO_2$, pyridine, CH_2Cl_2, DMF, PhF, PhCl, and PhBr) illustrates examples of paramagnetic (or diamagnetic, depending on the trivalent metal M^{III} employed) molecular metals or superconductors.[3,6] Moreover, the ability of tris(oxalato)metalate complexes to form extended 2-D anionic layers in the presence of divalent metal ions has also been exploited for the preparation of the first molecular metal ferromagnets: $(ET)_3[Mn^{II}Cr^{III}(C_2O_4)_3]$ and $(BETS)_x[Mn^{II}Cr^{III}(C_2O_4)_3]\cdot CH_2Cl_2$ (BETS = bis(ethylenedithio)tetraselenafulvalene; $x \approx 3$).[5] All these examples clearly show the ability of tris(oxalato)metalate complexes to work as convenient frameworks in the design of new TTF-based charge-transfer salts with novel solid-state properties.

Most of the work reported so far on the above kind of hybrid salts has been focused on the ET donor, which forms salts with a marked 2-D electronic character due to the side to side connectivity in the derived solids by S···S short contacts. As far as we know, besides ET, only the donor TTF has been combined to date with the $[M(C_2O_4)_3]^{3-}$ anions.[7] The selenium derivatives of ET can also provide interesting examples of hybrid salts as the substitution of S by the more diffuse Se atom has often shown an enhancement of the intermolecular chalcogen−chalcogen contacts and hence the conductivity of the solid.[8]

We report here on the preparation, crystal structures, and solid-state properties of five new radical salts prepared with the selenium-containing donor bis(ethylenediseleno)tetrathiafulvalene (BEST) and paramagnetic tris(oxalato)metalate anions: $(BEST)_4[M(C_2O_4)_3]\cdot PhCOOH\cdot H_2O$ with M^{III} = Cr (**1**) or Fe (**2**), $(BEST)_4[M(C_2O_4)_3]\cdot 1.5H_2O$ with M^{III} = Cr (**3**) or Fe (**4**), and $(BEST)_9[Fe(C_2O_4)_3]_2\cdot 7H_2O$ (**5**). A preliminary report of these salts has already been published.[9]

Experimental Section

Synthesis. The organic donor bis(ethylenediseleno)tetrathiafulvalene (BEST) was synthesized as described in the literature.[10] Tris(oxalato)metalate(III) potassium salts, $K_3[M(C_2O_4)_3]\cdot 3H_2O$ (M = Fe, Cr), were also prepared as previously reported[11] and recrystallized several times from water. Benzonitrile (Fluka, 99%) and 18-crown-6 ether (Fluka, 99%) were used as received. The radical salts were prepared by electrochemical oxidation of the donor on platinum wire electrodes in U-shaped cells under low constant current. The anodic and cathodic compartments are separated by a porous glass frit. The exact conditions for the synthesis of each particular radical salt are described below.

Synthesis of $(BEST)_4[M(C_2O_4)_3]\cdot PhCOOH\cdot H_2O$, M^{III} = Cr (1) and Fe (2). A solution of racemic $K_3[M(C_2O_4)_3]\cdot 3H_2O$ (5 mM) and 18-crown-6 ether (1.5×10^{-2} M) in 20 mL of benzonitrile and 2 mL of methanol was distributed between the two compartments of a U-shaped cell. Solid BEST (8 mg) was introduced in the anode compartment, and a constant current of 1 μA was applied during 20 days and then 2 μA during 4 days more for **1**. In the case of salt **2**, a current of 1.5 μA was applied during 9 days. Both salts were collected as dark needles.

Synthesis of $(BEST)_4[M(C_2O_4)_3]\cdot 1.5H_2O$, M^{III} = Cr (3) and Fe (4). A solution of racemic $K_3[M(C_2O_4)_3]\cdot 3H_2O$ (5 mM) and 18-crown-6 ether (1.5×10^{-2} M) in 20 mL of anhydrous benzonitrile and 2 mL of methanol (this last solvent only for **3**) was distributed between the two compartments of a U-shaped cell. Solid BEST (8 mg) was introduced in the anode compartment, and a constant current of 1 μA was applied. Dark needles of compounds **3** and **4** were collected after 1 week.

Synthesis of $(BEST)_9[Fe(C_2O_4)_3]_2\cdot 7H_2O$ (5). A solution of racemic $K_3[Fe(C_2O_4)_3]\cdot 3H_2O$ (5 mM) and 18-crown-6 ether ($1.5 \times 10^{-}2$ M) in 20 mL of anhydrous benzonitrile was prepared and distributed between the two compartments of a U-shaped cell. Solid BEST (8 mg) was added to the anode compartment, and a constant current of 0.3 μA was applied between the platinum electrodes. Dark needles of compound **5** were collected after 2 weeks.

Structure Determination. The crystal structures of compounds **1**−**3** and **5** were determined from single-crystal X-ray diffraction data collected at 150(2) K for **2**, **3**, and **5** and at 293(2) K for **1**. Compound **4** was found to be isostructural to **3** by the determination of the unit cell parameters of a single crystal. Data were collected with a Nonius KappaCCD diffractometer using a graphite-monochromated Mo Kα radiation source (λ = 0.710 73 Å). Denzo and Scalepack[12] programs were used for cell refinements and data reduction. The structures were solved by direct methods using the SIR97[13] program with the WinGX[14] graphical user interface. The structure refinements were carried out with SHELX-97.[15] A

(3) (a) Graham, A. W.; Kurmoo, M.; Day, P. *J. Chem. Soc., Chem. Commun.* **1995**, 2061. (b) Kurmoo, M.; Graham, A. W.; Day, P.; Coles, S. J.; Hursthouse, M. B.; Caulfield, J. L.; Singleton, J.; Pratt, F. L.; Hayes, W.; Ducasse, L.; Guionneau, P. *J. Am. Chem. Soc.* **1995**, *117*, 12209. (c) Martin, L.; Turner, S. S.; Day, P.; Mabbs, F. E.; McInnes, E. J. L. *Chem. Commun.* **1997**, 1367. (d) Rashid, S.; Turner, S. S.; Day, P.; Howard, J. A. K.; Guionneau, P.; McInnes, E. J. L.; Mabbs, F. E.; Clark, R. J. H.; Firth, S.; Biggs, T. *J. Mater. Chem.* **2001**, *11*, 2095. (e) Coronado, E.; Curreli, S.; Giménez-Saiz, C.; Gómez-García, C. J. *J. Mater. Chem.* **2005**, *15*, 1429.

(4) (a) Kobayashi, H.; Kobayashi, A.; Cassoux, P. *Chem. Soc. Rev.* **2000**, *29*, 325. (b) Fujiwara, H.; Fujiwara, E.; Nakazawa, Y.; Narymbetov, B. Zh.; Kato, K.; Kobayashi, H.; Kobayashi, A.; Tokumoto, M.; Cassoux, P. *J. Am. Chem. Soc.* **2001**, *123*, 306.

(5) (a) Coronado, E.; Galán-Mascarós, J. R.; Gómez-García, C. J.; Laukhin, V. N. *Nature (London)* **2000**, *408*, 447. (b) Alberola, A.; Coronado, E.; Galán-Mascarós, J. R.; Giménez-Saiz, C.; Gómez-García, C. J. *J. Am. Chem. Soc.* **2003**, *125*, 10774.

(6) (a) Turner, S. S.; Day, P.; Abdul Malik, K. M.; Hursthouse, M. B.; Teat, S. J.; MacLean, E. J.; Martin, L.; French, S. A. *Inorg. Chem.* **1999**, *38*, 3543. (b) Akutsu, H.; Akutsu-Sato, A.; Turner, S. S.; Le Pevelen, D.; Day, P.; Laukhin, V.; Klehe, A.-K.; Singleton, J.; Tocher, D. A.; Provert, M. R.; Howard, J. A. K. *J. Am. Chem. Soc.* **2002**, *124*, 12430. (c) Rashid, S.; Turner, S. S.; Le Pevelen, D.; Day, P.; Light, M. E.; Hursthouse, M. B.; Firth, S.; Clark, R. J. H. *Inorg. Chem.* **2001**, *40*, 5304. (d) Prokhorova, T. G.; Khasanov, S. S.; Zorina, L. V.; Buravov, L. I.; Tkacheva, V. A.; Baskakov, A. A.; Morgunov, R. B.; Gener, M.; Canadell, E.; Shibaeva, R. P.; Yagubskii, E. B. *Adv. Funct. Mater.* **2003**, *13*, 403.

(7) (a) Coronado, E.; Galán-Mascarós, J. R.; Giménez-Saiz, C.; Gómez-García, C. J.; Ruiz-Pérez, C.; Triki, S. *Adv. Mater.* **1996**, *8*, 737. (b) Clemente-León, M.; Coronado, E.; Galán-Mascarós, J. R.; Giménez-Saiz, C.; Gómez-García, C. J.; Fabre, J. M. *Synth. Met.* **1999**, *103*, 2279. (c) Coronado, E.; Galán-Mascarós, J. R.; Giménez-Saiz, C.; Gómez-García, C. J.; Ruiz-Pérez, C. *Eur. J. Inorg. Chem.* **2003**, 2290. (d) Coronado, E.; Galán-Mascarós, J. R.; Giménez-Saiz, C.; Gómez-García, C. J.; Martínez-Agudo, J. M.; Martínez-Ferrero, E. *Polyhedron* **2003**, *22*, 2381.

(8) Williams, J. M.; Ferraro, J. R.; Thorn, R. J.; Carlson, K. D.; Geiger, U.; Wang, H. H.; Kini, A. M.; Whangbo, M. H. *Organic Superconductors: Synthesis, Structure, Properties and Theory*; Crimes, R. N., Ed.; Prentice Hall: Englewood Cliffs, NJ, 1992.

(9) Coronado, E.; Curreli, S.; Giménez-Saiz, C., Gómez-García, C. J. *Synth. Met.* **2005**, *154*, 245.

(10) Kini, A. M.; Gates, B. D.; Beno, M. A.; Williams, J. M. *Chem. Commun.* **1989**, 169.

(11) Palmer, W. G. *Experimental Inorganic Chemistry*; Cambridge University Press: Cambridge, U.K., 1954.

Table 1. X-ray Crystallographic Data for $(BEST)_4[M(C_2O_4)_3]\cdot PhCOOH\cdot H_2O$ with M^{III} = Cr (**1**) or Fe (**2**), $(BEST)_4[M(C_2O_4)_3]\cdot 1.5H_2O$ with M^{III} = Cr (**3**) or Fe (**4**), and $(BEST)_9[Fe(C_2O_4)_3]_2\cdot 7H_2O$ (**5**)

param	**1**	**2**	**3**	**4**[b]	**5**
chem formula	$C_{53}H_{40}CrO_{15}S_{16}Se_{16}$	$C_{53}H_{40}FeO_{15}S_{16}Se_{16}$	$C_{46}H_{35}CrO_{13.5}S_{16}Se_{16}$	$C_{46}H_{35}FeO_{13.5}S_{16}Se_{16}$	$C_{102}H_{86}Fe_2O_{31}S_{36}Se_{36}$
a (Å)	14.0999(4)	14.0326(3)	33.7480(10)	33.659(6)	12.6993(3)
b (Å)	15.3464(4)	15.1981(4)	12.3151(7)	12.248(2)	18.7564(4)
c (Å)	19.5000(4)	19.4106(4)	8.8218(5)	8.759(2)	18.7675(4)
α (deg)	76.711(5)	76.739(5)	90	90	75.649(5)
β (deg)	71.688(5)	71.938(5)	99.674(5)	99.74(3)	107.178(5)
γ (deg)	88.545(5)	88.845(5)	90	90	79.527(5)
V (Å^3)	3893.5(2)	3824.9(2)	3614.3(3)	3558.9(12)	3977.5(3)
T/K	293(2)	150(2)	150(2)	150(2)	150(2)
Z	2	2	2		1
fw	2745.17	2749.02	2632.06		5916.13
cryst syst	triclinic	triclinic	monoclinic		triclinic
space group	$P\bar{1}$	$P\bar{1}$	*C*2/*m*		$P\bar{1}$
ρ_{calcd}/g cm^{-3}	2.342	2.387	2.419		2.470
μ/mm^{-1}	8.115	8.308	8.734		8.959
$R(F_o)$, $R_w(F_o^2)$ [$I < 2\sigma(I)$][a]	0.0598, 0.1368	0.0688, 0.1656	0.0817, 0.2429		0.0684, 0.1769

[a] $R = \sum(F_o - F_c)/\sum F_o$. $R_w = \{\sum[w(F_o^2 - F_c^2)^2]/\sum[w(F_o^2)^2]\}^{1/2}$. [b] Only the cell parameters were obtained for this compound.

multiscan absorption correction, based on equivalent reflections, was applied to the data using the program SORTAV.[16] All non-hydrogen atoms were refined anisotropically. Hydrogen atoms on carbon atoms were included at calculated positions and refined with a riding model. Hydrogen atoms of water molecules or hydroxonium ions were not located. Crystal data are listed in Table 1.

Conductivity Measurements. Dc conductivity measurements over the temperature range 2−300 K were performed with the four contacts method for several single crystals of each salt, giving reproducible results in all the samples. The contacts between the platinum wires (25 μm diameter) and the samples were done using graphite paste. All the samples were measured with cooling and warming rates of 1 K min^{-1} and with dc intensity currents of 1 μA in a Quantum Design PPMS-9.

Magnetic Measurements. Variable-temperature susceptibility measurements were carried out in the temperature range 2−300 K with an applied magnetic field of 0.1 T on polycrystalline samples of **1**, **2**, **4**, and **5** with a Quantum Design MPMS-XL-5 SQUID magnetometer. The synthesis of sample **3** yielded only a few crystals, precluding the performance of reliable magnetic measurements. ESR spectra were recorded in X band (ν = 9.79 GHz) with a Bruker ELEXSYS E-500 spectrometer in the temperature range 300−3 K on polycrystalline and single-crystal samples.

Results and Discussion

Synthesis. Three different phases are obtained when the BEST molecule is associated with tris(oxalato)metalate(III) anions using the electrocrystallization method and benzonitrile as solvent. One of these phases (compounds **1** and **2**) contain benzoic acid molecules in its crystal structure, although no benzoic acid was used as starting material in the electrocrystallization process. It seems that the PhCOOH molecules come from a hydrolysis reaction (Scheme 1) of some of the benzonitrile molecules. This hydrolysis is probably due to the aging of the wet solvent (which stood on the shelf for several years).

Scheme 1

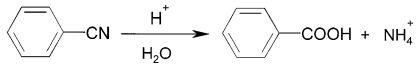

When a recently distilled and anhydrous benzonitrile solvent was used, two phases that do not contain benzoic acid (compounds **3**−**5**) were obtained.

The isostructural compounds **3** and **4** are obtained when using a higher current intensity (1 μA) than for compound **5** (0.3 μA). This difference is in agreement with the donor:anion ratio of the salts (4:1 for **3** and **4** and 9:2 for **5**) since a lower current intensity generally implies a slower oxidation rate of the organic donor and, therefore, a higher rate between neutral and charged ET molecules (in average 2:6 in salts **3** and **4** and 3:6 in salt **5**) or, in other words, a lower value of the average charge/donor (+3/4 in salts **3** and **4** and +2/3 in salt **5**).

Crystal Structures. As mentioned in the Introduction, several phases of conducting radical salts of the ET donor containing magnetic tris(oxalato)metalate anions have been previously reported.[3,5,6] In these phases, the layers containing the tris(oxalato)metalate anions generally exhibit a common structural pattern due to the supramolecular bonding capacity of these anions which can form coordinate bonds using the terminal oxygen atoms of the oxalate ligands (since they are not bonded to the central trivalent metal). This structural pattern consists of triangular two-dimensional arrays of the tris(oxalato)metalate anions having their trigonal axes perpendicular to the layers. The anions are separated by H_3O^+, K^+, or NH_4^+ cations as in the monoclinic series of superconductors $(ET)_4[(H_3O)M(C_2O_4)_3]\cdot G$ (see Figure 1a) or the orthorhombic series of semiconductors $(ET)_4[A^IM^{III}(C_2O_4)_3]\cdot PhCN$ (see Figure 1b). The whole forms a pseudohexagonal lattice very similar to that found in bimetallic tris(oxalate) salts with organic cations such as NBu_4^+ or even the ET donor in the ferromagnetic metal $(ET)_3[Mn^{II}Cr^{III}(C_2O_4)_3]$ (Figure 1c). The relevance of the anionic distribution can be noted in the series $(ET)_4[(H_3O)M(C_2O_4)_3]\cdot G$, in which it

(12) Otwinowski, Z.; Minor, W. DENZO-SCALEPACK, Processing of X-ray Diffraction Data Collected in Oscillation Mode. In *Methods in Enzymology, Volume 276, Macromolecular Crystallography*; Carter, C. W., Jr., Sweet, R. M., Eds.; Academic Press: New York, 1997; Part A.
(13) Altomare, A.; Burla, M. C.; Camalli, M.; Cascarano, G.; Giacovazzo, C.; Guagliardi, A.; Moliterni, A. G. G.; Polidori, G.; Spagna, R. *J. Appl. Crystallogr.* **1999**, *32*, 115.
(14) Farrugia, L. J. *J. Appl. Crystallogr.* **1997**, *32*, 837.
(15) Sheldrick, G. M. *SHELX-97*; University of Göttingen: Göttingen, Germany, 1997.
(16) Blessing, R. H. *J. Appl. Crystallogr.* **1997**, *30*, 421.

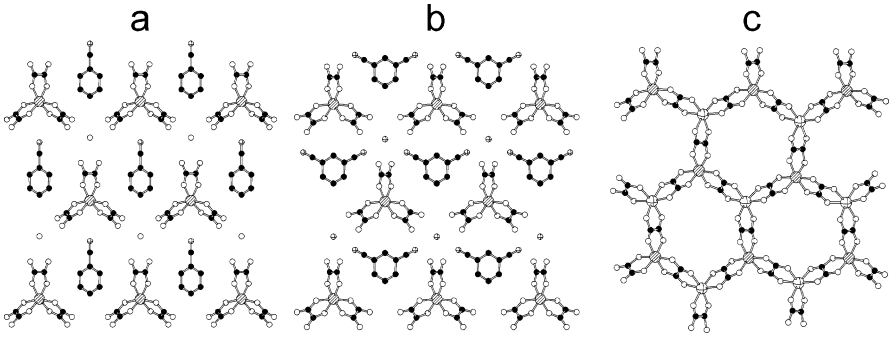

Figure 1. Comparison of the anionic layers of the radical salts $(ET)_4[(H_3O)Fe(C_2O_4)_3]\cdot PhCN$ (a), $(ET)_4[(NH_4)Fe(C_2O_4)_3]\cdot PhCN$ (b), and $(ET)_3[MnCr(C_2O_4)_3]$ (c). The carbon atoms are depicted as black spheres, the oxygen atoms as white spheres, the nitrogen atoms as crossed spheres, and the metal atoms as hatched spheres.

has been suggested that this kind of pseudohexagonal 2-D anionic lattice influences the packing mode of the donor via short atomic contacts, i.e., H-bonding between the ET terminal ethylene groups and the O atoms of $[M(C_2O_4)_3]^{3-}$ anions.

When the tris(oxalato)metalate anions are combined with other TTF-type donors, as the seleniated BEST molecule, it could be expected to obtain layered compounds in which the anions distribute forming pseudohexagonal layers similar to the previously described (Figure 1). However, the anionic layers present in the BEST radical salts are very different. In salts **1** and **2**, the anion distribution is altered by the inclusion of PhCOOH molecules in the layer which form H-bonds with the oxygen atoms of the anions. In contrast, salts **3** and **4** do not contain PhCOOH molecules or other organic guest molecules in the anionic layers. Despite the fact that these salts have the same (4:1) cation:anion stoichiometry than the radical salts of the ET donor, the anion distribution is very different and is complicated by disorder. The pseudohexagonal arrangement of the anions is lost probably because the BEST donor has a larger molecular volume than the ET molecule, causing the anions to be more separated (in average) and thus avoiding the coordination of H_2O molecules (or H_3O^+ or K^+ cations if it was the case) by three anions at the same time, as it happens in the anionic layers shown in Figure 1a,b. This larger separation between the anions can be realized considering the area available/anion in the inorganic layers. In the series $(ET)_4[(H_3O)M(C_2O_4)]\cdot G$ this area ranges between 101 and 104 Å^2 (depending on the particular M ion and G molecule) compared to 108.2 Å^2 in **1** and 108.6 Å^2 in **3**. This expansion effect is more evident in the radical salt **5** (with a cation: anion stoichiometry of 9:2) in which the area available/anion is larger (117.1 Å^2) and therefore the anions are even more separated in average.

Crystal Structure of $(BEST)_4[M(C_2O_4)_3]\cdot PhCOOH\cdot H_2O$, M^{III} = Cr (1) and Fe (2). Compounds **1** and **2** are isostructural as found by the determination of their structures by single-crystal X-ray analysis. Table 1 contains the relevant crystallographic data and collection parameters. Figure 2 shows a standard ORTEP[17] diagram of the molecules of **1** with 50% thermal ellipsoids and atom numbering scheme.

The structures of these salts consist of layers of organic donors (parallel to the *ab* plane) alternating with layers formed by tris(oxalato)metalate anions, benzoic acid, and water molecules (Figure 3a). The organic layers are made up of four crystallographycally independent BEST molecules (labeled A−D) that are packed forming chains running along the [120] direction in which the BEST molecules exhibit the usual "face-to-face" stacking, giving rise to the so-called β phase (Figure 4a). In the stacks the BEST molecules arrange following the sequence ···ABCDDCBA··· (Figure 5a) and form tetramers in which each donor is slightly displaced respect to the next donor along the long molecular axis by 1.35 Å (in the pairs of molecules AB and BC) or 0.9 Å (in the pair CD). These displacements produce the typical "ring-over-bond" (RB) overlap mode inside the tetramer. Between each tetramer a "dislocation" appears consisting in a larger displacement along the long molecular axis (4.8 and 4.2 Å in the pairs AA and DD, respectively) producing another RB overlap between these molecules. Consequently the organic packing in **1** and **2** can be designated as β_{82} according to the clasification made by Mori[18] (the repeating unit is 8 with 2 dislocations, a unit cell involving 8 donor molecules).

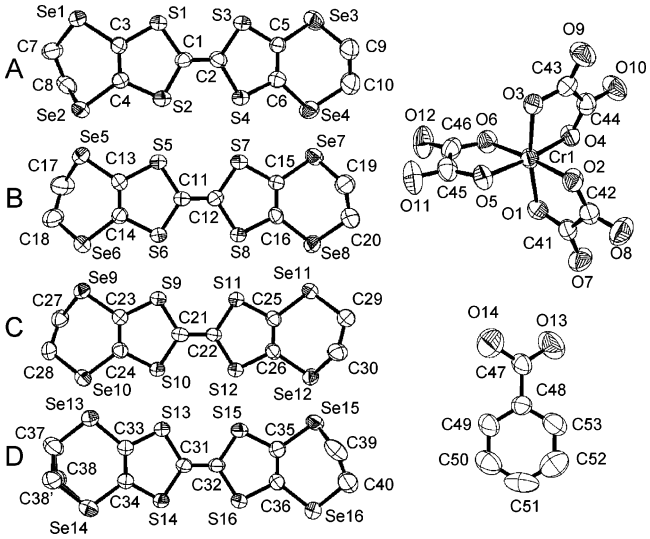

Figure 2. ORTEP diagram with 50% thermal ellipsoids and the atom numbering scheme for compound **1**, $(BEST)_4[Cr(C_2O_4)_3]\cdot PhCOOH\cdot H_2O$. The atom numbering scheme for the isostructural salt **2** is similar.

(17) Farrugia, L. J. *J. Appl. Crystallogr.* **1997**, *30*, 565.
(18) Mori, T. *Bull. Chem. Soc. Jpn.* **1998**, *71*, 2509.

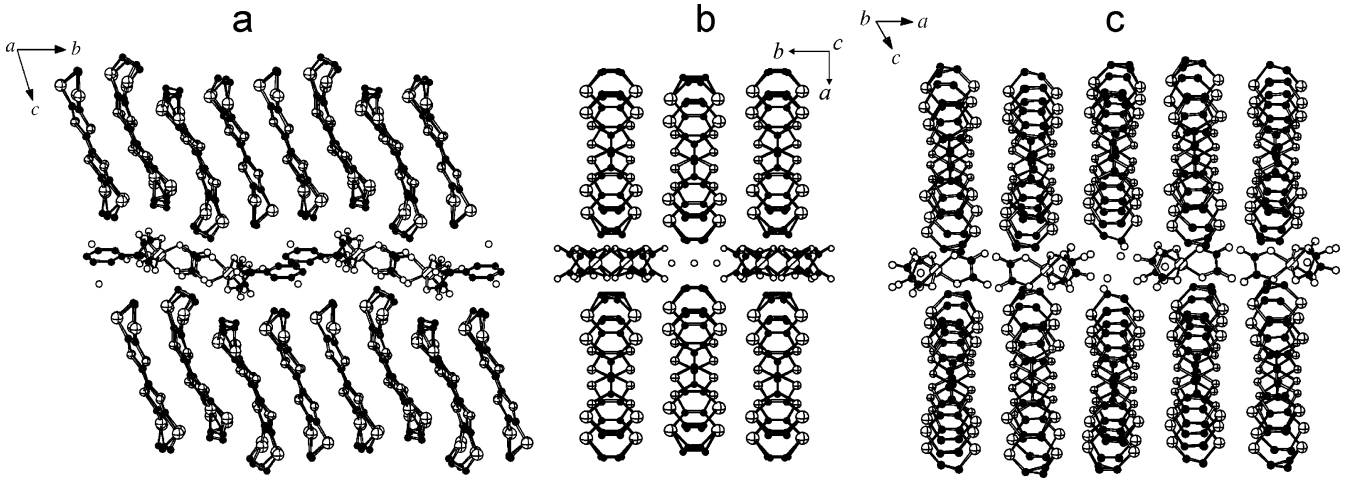

Figure 3. View of the alternating layers of organic donors and tris(oxalato)metalate anions in compounds **1** (a), **3** (b), and **5** (c). The carbon atoms are depicted as black spheres, the sulfur atoms as small crossed spheres, the selenium atoms as bigger crossed spheres, the oxygen atoms as white spheres, and the metal atoms (Cr or Fe) as hatched spheres.

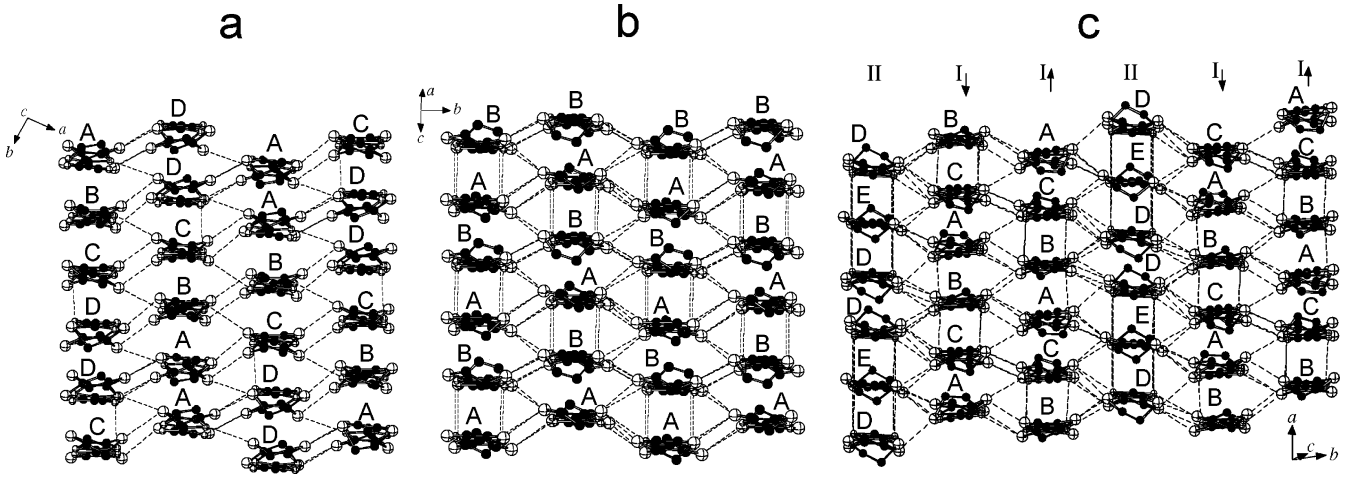

Figure 4. View of the organic layers of compounds **1** (a), **3** (b), and **5** (c), showing the β type of packing. The labeling of the crystallographically independent BEST molecules is shown. In (c) the roman numerals indicate the existence of different types of stacks (see text). The carbon atoms are depicted as black spheres, the sulfur atoms as small crossed spheres, and the selenium atoms as bigger crossed spheres. Dotted lines represent S···S, Se···S, and Se···Se intermolecular contacts shorter that the sum of the van der Waals radii. These intermolecular distances can be found as Supporting Information.

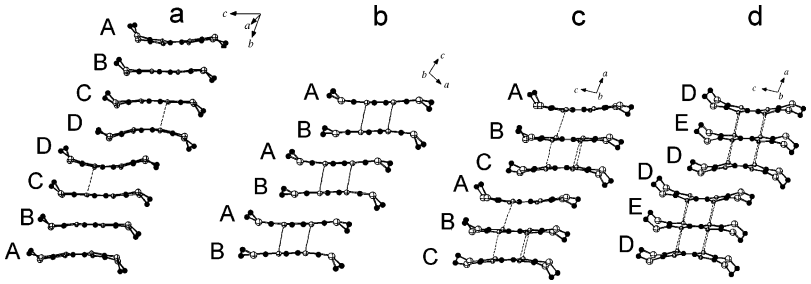

Figure 5. Comparison of the different stacks of BEST molecules occurring in the radical salts **1** (a), **3** (b), and **5** (c, d), showing the formation of tetramers, dimers, and trimers, respectively. The labeling of the crystallographically independent BEST molecules is shown. The carbon atoms are depicted as black spheres, the sulfur atoms as small crossed spheres, and the selenium atoms as bigger crossed spheres. Dotted lines represent the intrastack S···S contacts shorter than the sum of the van der Waals radii (all distances can be found as Supporting Information).

Molecule D shows one ethylene group disordered between two different positions. In **1** these disordered positions correspond to two boat conformations while in **2** one position corresponds to a boat conformation and the other to a sofa conformation.[19] All the other ethylene groups in both compounds are ordered and correspond to boat conformations. Of the three possible conformations that the ethylene groups can adopt (Figure 6) the boat conformation has been found to be the most stable for BEST molecules using ab initio calculations.[20] The staggered conformation has not been found yet in BEST salts,[21] although it is usually found in ET salts.

(19) The designation of the conformation of the ethylene groups has been made according to the definitions reported by the following: Matsumiya, S.; Izuoka, A.; Sugawara, T.; Taruishi, T.; Kawada, Y. *Bull. Chem. Soc. Jpn.* **1993**, *66*, 513.

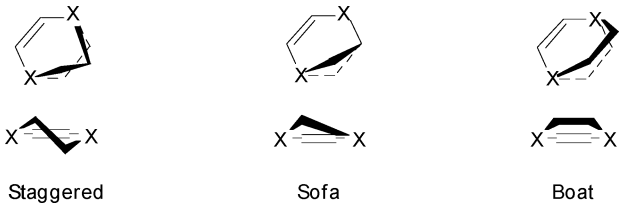

Figure 6. Schematic representation of the three possible conformations adopted by the six-membered rings of BEST (X = Se) and ET (X = S).

In the organic layer there are numerous short intermolecular chalcogen···chalcogen contacts which are shorter than the sum of the van der Waals radii. As usual in other BEST salts, S···S short contacts are only found inside the stacks, while the interstack short contacts are all of the type S···Se or Se···Se (see Supporting Information).

The estimation of the ionic charges on the BEST molecules from the known correlations between the intramolecular distances of the central TTF skeleton and the oxidation degree[22] indicates that the BEST molecules of A and C types are completely ionized, while B and D molecules have a charge of +1/2. This charge distribution agrees with the stoichiometry of the radical salt (one BEST molecule of each type/formula and one anion charged −3).

The anionic layer is formed by the chiral $[M(C_2O_4)_3]^{3-}$ units, PhCOOH molecules, and water molecules (Figure 7a). The tris(oxalato)metalate anions form zigzag rows along the *a* direction consisting of alternating Λ and Δ enantiomers. These zigzag rows are separated by benzoic acid and water molecules which form hydrogen bonds with the oxalate terminal oxygens. Although the acidic proton in PhCOOH has not been found in the crystal structure solution process, its presence is evidenced by the short distances between the oxygen atoms of PhCOOH and some oxygen atoms of the anion, which are typical of hydrogen bond formation. These distances (see Figure 7a) indicate that both oxygen atoms in PhCOOH (O13 and O14) participate in the hydrogen bonds, and therefore, the acidic hydrogen must be disordered over the two positions which correspond to the hydroxyl group in O13 or O14. This is supported by the similarity in the C47−O bond distances for O13 and O14 (1.348(9) and 1.368(9) Å for **1**; 1.352(11) and 1.319(11) Å for **2**). A similar disorder of the hydrogen atoms participating in the hydrogen bonds was also found in the crystal structure of benzoic acid which was studied by single-crystal neutron diffraction.[23] The water molecules are also involved in hydrogen bonding formation between them and also with the terminal oxygen atoms of the oxalate ligands (Figure 7a). Two types of contacts are established between the organic and the inorganic sublattices: contacts between the organic BEST and the anionic oxalates of the type Se···O (ranging between 2.905(5) and 3.234(6) for **1**), which are shorter than the sum of the van der Waals radii, and also numerous weak van der Waals interactions (2.30−3.00 Å) between the terminal ethylene hydrogens and oxygens of the oxalate.

Crystal Structure of $(BEST)_4[M(C_2O_4)_3]\cdot 1.5H_2O$, M^{III} = Cr (3) and Fe (4). Only the structure of the Cr^{III} derivative (**3**) has been solved. Compound **4** was found to be isostructural to **3** by the determination of its unit cell parameters from single-crystal X-ray diffraction analyses. Table 1 contains the relevant crystallographic data and collection parameters.

The asymmetric unit of **3** contains two half-BEST molecules lying on a reflection plane, 1/4 $[Cr(C_2O_4)_3]^{3-}$ entity lying on a 2-fold rotation axis (and also near an inversion center, causing a disorder in the anion; see below), and two water molecules having refined partial occupancies of less that unity (0.25 and 0.125). Figure 8 shows a standard ORTEP diagram of the molecules in **3** with 50% thermal ellipsoids and atom numbering scheme.

The crystal structure consists of alternating layers parallel to the *bc* plane (see Figure 3b) containing only BEST molecules in the organic layers and only tris(oxalato)metalate anions and water in the inorganic layers. As in salts **1** and **2**, the BEST molecules exhibit a "face-to-face" stacking and a RB overlap mode giving rise to a β-packing (Figure 4b). However, the arrangement of the donors in the stacks is different from the one found in **1** and **2**. Now there are only two crystallographically different BEST molecules (labeled A and B) which stack forming dimers in the *c* direction and follow the sequence ···AB··· (Figure 5b). In these stacks the molecules forming the dimers are slighly displaced along the long molecular axis by ca. 0.80 Å, while different dimers are displaced by a longer distance of ca. 4.29 Å. Therefore, this kind of packing can be designated (according to Mori)[18] as $\beta_{21\times2}$. (The repeating unit is 2 with 1 dislocation, and there are two β_{21} chains along the transverse direction.) Accordingly, a unit cell contains $2 \times 2 = 4$ donor molecules/layer, i.e., 8 donor molecules/unit cell (since there are two layers/unit cell).

Every ethylene group of the BEST molecules is disordered between two different positions (see Figure 8). In molecule A all the disordered positions correspond to boat conformations, while in molecule B the two disordered positions of one side of the molecule (C11−C11′) adopt a boat conformation and in the other side (C12−C12′) the two disordered positions adopt a sofa conformation.[19]

As in compounds **1** and **2**, the only intrastack short contacts are all of the type S···S (found between the molecules forming the dimers) while the S···Se and Se···Se short contacts are found between different stacks (see Supporting Information).

The crystallographically independent BEST molecule of type A has a positive charge close to +1, while the B-type BEST molecule has a charge of +1/2, as estimated from the bond lengths using the relationship of Guionneau et al.[22]

(20) Wang, J. H.; Montgomery, L. K.; Geiser, U.; Porter, L. C.; Carlson, K. D.; Ferraro, J. R.; Williams, J. M.; Cariss, C. S.; Rubinstein, R. L.; Whitworth, J. R.; Evain, M.; Novoa, J. J.; Whangbo, M.-H. *Chem. Mater.* **1989**, *1*, 140.

(21) This conclusion has been reached by examination of all the crystal structures containing the BEST donor that are deposited in the Cambridge Structural Database.

(22) Guionneau, P.; Kepert, C. J.; Bravic, G.; Chasseau, D.; Truter, M. R.; Kurmoo, M.; Day, P. *Synth. Met.* **1997**, *86*, 1973. Although this method was devised for ET molecules, it may also be applied for the BEST molecules due to the similarity of the central skeleton of both molecules.

(23) Wilson, C. C.; Shankland, N.; Florence, A. J. *J. Chem. Soc., Faraday Trans.* **1996**, *92*, 5051.

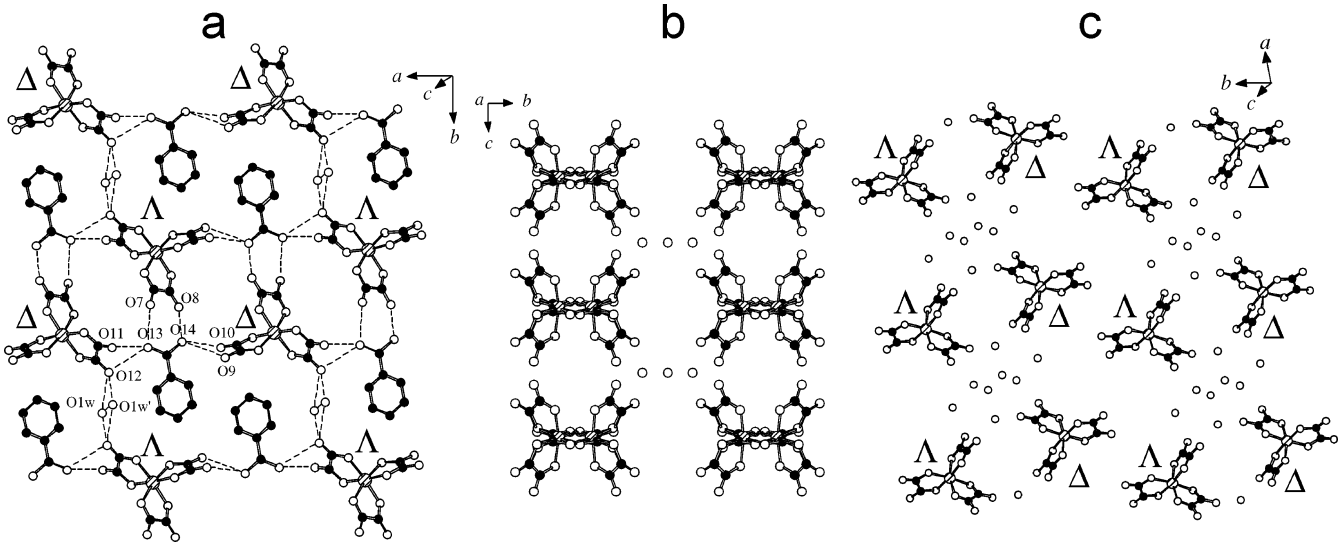

Figure 7. Comparison of the anionic layers of **1** (a), **3** (b), and **5** (c). The carbon atoms are depicted as black spheres, the oxygen atoms as white spheres, and the metal atoms (Cr or Fe) as hatched spheres. Dotted lines in (a) represent hydrogen bond formation (see text). The relevant distances are O7···O13 = 2.926(9) Å, O8···O14 = 2.745(9) Å, O11···O13 = 2.893(9) Å, O12···O13 = 3.166(9) Å, O9···O14 = 3.566(9) Å, O10···O14 = 2.705(9) Å, O1w···O12 = 2.958(12) Å, O1w′···O12 = 2.867(11) Å, and O1w···O1w′ = 3.169(19) Å.

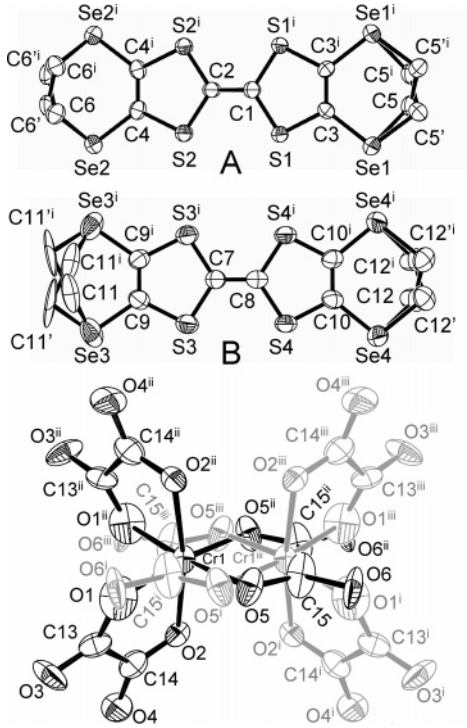

Figure 8. ORTEP diagram with 50% thermal ellipsoids and the atom numbering scheme for compound **3**, $(BEST)_4[Cr(C_2O_4)_3]\cdot 1.5H_2O$. The disorder found in the anion is shown (see text). Symmetry codes: (i) $x, -y + 1, z$; (ii) $-x + 1, y, -z + 2$; (iii) $-x + 1, -y + 2, -z + 2$.

This charge distribution agrees with the stoichiometry of the radical salt (two BEST molecules of each type/formula and one anion charged −3).

The inorganic layer comprises tris(oxalato)metalate anions and water molecules. The anions exhibit a disorder of the whole anion over two possible positions which are separated 2.283 Å along the 2-fold axis (parallel to the *b* axis). Therefore, this disorder makes the anion to appear as two interpenetrated anions (see Figure 8). This kind of disorder in the anionic part is not unusual in radical salts of TTF-based donors containing complex anions. For example, similar (not resolved) disorders have also been observed in the radical salts $(BETS)_4[Fe(CN)_5NO]$,[24] $(BEDO)_4[Fe(CN)_5NO]$,[25] $(BET)_4(NEt_4)_2[Fe(CN)_6]$,[26] and $(ET)_3[MnCr(C_2O_4)_3]$.[5a] In the present case the disorder of the anion has been completely resolved over two interpenetrated positions. The disordered anions are placed in rows parallel to the *c* axis, and the water molecules, having partial occupancies, are located between these rows (Figure 7b).

As in the previous salts, there are short contacts between the inorganic and the organic sublattices of Se···O type with oxygen atoms of the anions or the water molecules (the contacts range between 3.027(18) and 3.23(3) Å).

Crystal Structure of $(BEST)_9[Fe(C_2O_4)_3]_2\cdot 7H_2O$ (5). The asymmetric unit of **5** contains one tris(oxalato)ferrate anion, five independent BEST molecules (one of them lying about an inversion center), and four water molecules, one of them having a refined occupancy of 0.5. The relevant crystallographic data and collection parameters are listed in Table 1. Figure 9 shows a standard ORTEP diagram of the molecules with 50% thermal ellipsoids and atom numbering scheme.

Compound **5** consists of alternating organic and inorganic layers parallel to the *ab* plane (Figure 3c). The five crystallographically independent BEST molecules have been labeled as A−E, with molecule E lying about an inversion center, whereas the rest are in general positions. As in the previous salts, the organic layers adopt the so-called β packing, although now there are two different kinds of

(24) Sanchez, M.-E.; Doublet, M.-L.; Faulmann, C.; Malfant, I.; Cassoux, P.; Kushch, L. A.; Yagubskii, E. B. *Eur. J. Inorg. Chem.* **2001**, 2797.
(25) Zorina, L. V.; Khasanov, S. S.; Shibaeva, R. P.; Gener, M.; Rousseau, R.; Canadell, E.; Kushch, L. A.; Yagubskii, E. B.; Drozdova, O. O.; Yakushi, K. *J. Mater. Chem.* **2000**, *10*, 2017.
(26) Clemente-León, M.; Coronado, E.; Galán-Mascarós, J. R.; Giménez-Saiz, C.; Gómez-García, C. J.; Ribera, E.; Vidal-Gancedo, J.; Rovira, C.; Canadell, E.; Laukhin, V. *Inorg. Chem.* **2001**, *40*, 3526.

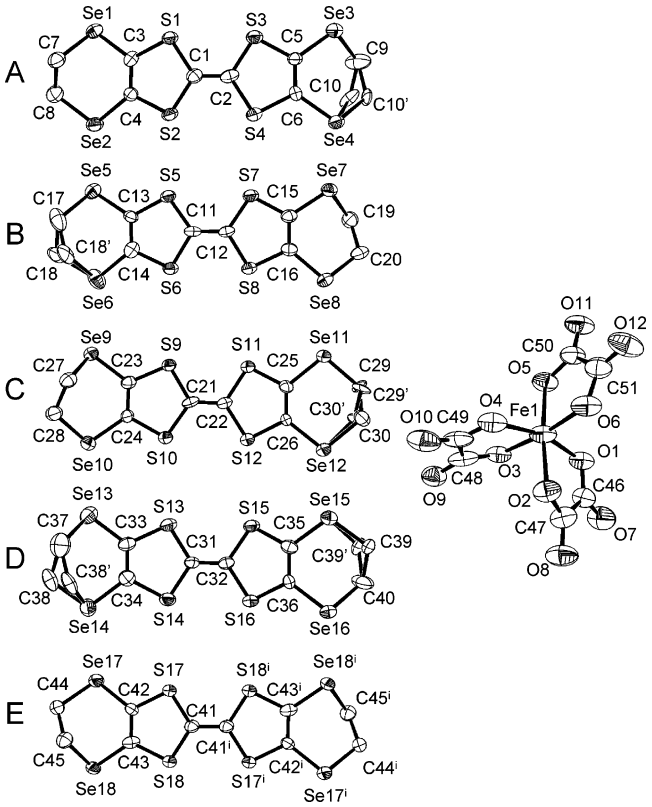

Figure 9. ORTEP diagram with 50% thermal ellipsoids and the atom numbering scheme for compound **5**, $(BEST)_9[Fe(C_2O_4)_3]_2 \cdot 7H_2O$. Symmetry code: (i) $-x + 1, -y, -z$.

organic stacks (labeled as I and II in Figure 4c) both having a repeating unit of three molecules: ···ABC··· and ···DED··· in stacks I and II, respectively. In addition, there are two stacks of type I (exhibiting the sequence in opposite directions: labeled as $I_\uparrow$ and $I_\downarrow$) alternating with one stack of type II in the *b* direction (Figure 4c). In both types of stacks the BEST molecules form trimers with a RB overlap mode inside the trimers (with displacement along the long molecular axis of ca. 1.3, 1.0, and 0.7 Å between the pairs AB, BC, and DE, respectively; see Figure 5c,d). Dislocations of ca. 4.4 and 4.5 Å (in stacks I and II, respectively) appear between different trimers. Therefore, the organic packing in **5** can be designated as $\beta_{31\times3}$ according to the clasification made by Mori.[18] (The repeating unit is 3 with 1 dislocation, and there are 3 β_{31} chains along the transverse direction; therefore, a unit cell involves $3 \times 3 = 9$ donor molecules.)

Disorder can be seen on one of the terminal ethylene groups on the A-, B-, and C-type BEST molecules and in both ethylene groups of molecule D. The ethylene group formed by C29−C30 (in molecule D) adopts a sofa conformation, while all the other ethylene groups adopt boat conformations.[19]

As in the previous salts, all the intrastack chalcogen··· chalcogen contacts shorter than the sum of the van der Waals radii are of the type S···S while the interstack contacts are of the type S···Se and Se···Se (see Supporting Information).

The analysis of the bond distances using the relationship of Guionneau et al.[22] also shows an inhomogeneous charge distribution in **5** for the five crystallographically independent BEST molecules, with charges of +0.3, +0.7, +0.5, +0.3, and +1.1 for molecules A−E, respectively. As there are two molecules of types A−D and one of type E per formula, the whole positive charge is estimated as $+4.7 \pm 0.9$, which suggests the presence of one proton in the inorganic layer to keep the electroneutrality as there are two tris(oxalato)-ferrate(III) anions/formula (each one with a charge of −3). Although this extra proton cannot be observed in the X-ray structure determination, the presence of up to seven water molecules/formula unit, which are involved in several H-bonds among them (see below), provides a possible location for this extra proton. Nevertheless, the low accuracy in the estimation of the charge of the BEST molecules precludes a definite charge assignment, and therefore, the presence of the extra proton cannot be certainly established. The presence of hydroxonium ions has often been proved in other radical salts of TTF-type donors, as for example in the related series of molecular superconductors containing the ET donor and tris(oxalato)metalate(III) anions formulated as $(ET)_4[(H_3O)M(C_2O_4)_3]\cdot G$,[3,6] and also in some polyoxometalate-containing radical salts.[27]

The anionic layer in **5** is formed by chiral $[Fe(C_2O_4)_3]^{3-}$ units and water molecules. As in the structures of **1** and **2**, the anions arrange forming zigzag rows, now parallel to the *b* direction, consisting of alternating Λ and Δ enantiomers (Figure 7c). However, in **5** the anions are more loosely packed than in **1** and **2**; i.e., the anions are more separated (the minimum distance between the metals in the *b* direction is 9.93 Å, compared to ca. 8.4 Å in **1** and **2**), therefore allowing for a increase in the number of donors/anion in the formula of salt **5**. The water molecules are located between the anionic rows and are involved in a network of H-bonding between them and also with some terminal oxygen atoms of the oxalate ligands. Thus, there are four O−H···O bridges between water molecules (O1w···O4w = 2.68(4) Å, O2w···O4w = 2.66(3) Å, O2w···O4w^{i} = 2.83(3) Å, O2w···O3w^{ii} = 2.84(3) Å) and three O−H···O bridges between water molecules and terminal oxalate oxygen atoms (O1w···O8 = 2.744(17) Å, O1w···O9^{iii} = 2.868(17) Å, O2w···O7 = 2.725(18) Å).[28]

The Se···O type contacts between the BEST donors and the anions are particularly short in this radical salt, ranging between 2.832(10) and 3.420(9) Å. Such short Se···O contacts have been observed in other radical salts with the BEST donor and anions presenting terminal oxygens, such as the polyoxometalate-containing radical salt $(BEST)_3H[PMo_{12}O_{40}]\cdot CH_3CN\cdot CH_2Cl_2$,[27] in which the Se···O contacts range between 2.95 and 3.15 Å.

Electrical Properties. The dc electrical conductivity for compounds **1**−**5** was measured on the best developed face of the single crystals, which is parallel to the donor layers. The temperature dependence of the conductivities of these radical salts is displayed in Figure 10. Note that below ca. 100 K for salt **5** and ca. 50 K for salts **1**−**4** the resistivity is

(27) Coronado, E.; Galán-Mascarós, J. R.; Giménez-Saiz, C.; Gómez-García, C. J.; Falvello, L. R.; Delhaès, P. *Inorg. Chem.* **1998**, *37*, 2183.
(28) Symmetry codes: (i) $-x, -y + 1, -z + 1$; (ii) $x - 1, y, z$; (iii) $-x + 1, -y + 1, -z + 1$.

Table 2. Electrical and Magnetic Properties of the Radical Salts **1**−**5**

compd	σ_{300K} (S cm^{-1})	E_a (meV)	C (emu K mol^{-1})	Θ (K)
(BEST)$_4$[Cr(C$_2$O$_4$)$_3$]·PhCOOH·H$_2$O (**1**)	1.5	49	1.856	−0.01
(BEST)$_4$[Fe(C$_2$O$_4$)$_3$]·PhCOOH·H$_2$O (**2**)	6.4	54	4.292	−0.77
(BEST)$_4$[Cr(C$_2$O$_4$)$_3$]·1.5H$_2$O (**3**)	8.5	62		
(BEST)$_4$[Fe(C$_2$O$_4$)$_3$]·1.5H$_2$O (**4**)	14.0	60	4.304	−1.1
(BEST)$_9$[Fe(C$_2$O$_4$)$_3$]$_2$·7H$_2$O (**5**)	2.4	44	4.270/Fe	−0.03

too high to be measured by our equipment. These compounds show a semiconducting behavior with high room-temperature conductivities (σ_{300K}), ranging from 2 to 20 S·cm^{-1}, and Arrhenius-like behaviors on decreasing the temperature with activation energies (E_a) between 44 and 62 meV (see Table 2). The semiconducting behavior can be explained by the presence of BEST molecules completely ionized in all the radical salts, breaking the electronic delocalization path along the stacks. The presence of chalcogen···chalcogen short contacts, however, accounts for the relatively high room-temperature values and the low activation energies.

Magnetic Susceptibility. The thermal variation of the product of the magnetic susceptibility times the temperature ($\chi_m T$) for compounds **1**−**3** and **5** is displayed in Figure 11. In all salts Curie−Weiss behavior is observed with Curie constants very close to those expected for Fe^{III} (4.375 emu K mol^{-1}, $S = 5/2$) or Cr^{III} (1.875 emu K mol^{-1}, $S = 3/2$) ions and with small values of the Weiss constants (see Table 2). These low Weiss constants account for the presence of very weak antiferromagnetic interactions between the Fe^{III} or Cr^{III} centers and/or the presence of a zero-field splitting in the Fe^{III} and Cr^{III} ions. On the other hand, no noticeable influence coming from the organic component on the

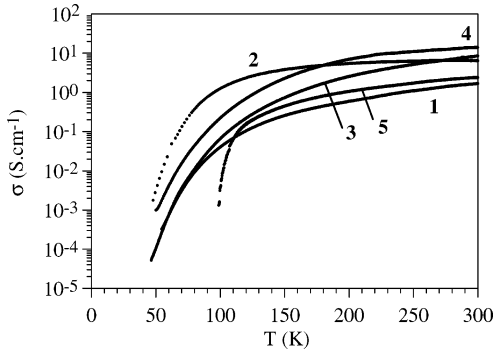

Figure 10. Thermal variation of the dc electrical conductivity on single crystals of the compounds **1**−**5**.

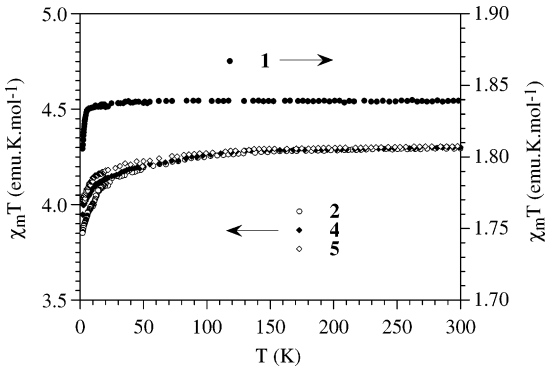

Figure 11. Thermal variation of the product of the molar magnetic susceptibility/metallic ion times the temperature ($\chi_m T$) for compounds **1**, **2**, **4**, and **5**.

magnetic moment is detected, suggesting that the localized spins on the BEST molecules must be strongly antiferromagnetically coupled, in agreement with the ESR spectroscopy results (see below).

The absence of a significant magnetic contribution coming from the organic sublattice is confirmed by electronic spin resonance (ESR) spectroscopy in the five compounds. At room temperature the five compounds show very similar ESR spectra with a weak and narrow feature at ca. 3400 G ($g_{BEST} = 2.004-2.006$) with line widths (ΔH) in the range 55−35 G, coming from some isolated BEST$^+$ radicals (due to impurities and crystal defects), and a more broad signal at ca. 1600−1800 G ($g_\perp = 3.60-4.48$) with ΔH in the range 180−230 G, coming from the magnetic [Fe(C$_2$O$_4$)$_3$]$^{3-}$ and [Cr(C$_2$O$_4$)$_3$]$^{3-}$ anions (Figure 12). When the temperature is lowered, the BEST signal decreases in intensity and below ca. 25−50 K it becomes almost negligible. This behavior indicates that the weak magnetic contribution of the BEST$^+$ radicals is canceled at low temperatures due to the presence of antiferromagnetic exchange interactions inside the organic sublattice. The signal at ca. 1600−1800 G increases its intensity in a paramagnetic way when decreasing the temperature, and at low temperatures a second broad signal at ca. 3300 G appears. This new broad signal, which is attributed to the parallel component ($g_{||}$) of the corresponding magnetic [Fe(C$_2$O$_4$)$_3$]$^{3-}$ and [Cr(C$_2$O$_4$)$_3$]$^{3-}$ anions, presents g values in the range 2.04−2.05 and line widths of 220−460 G (Figure 12). Note that the intensity of the broad signals coming from the magnetic anions is much higher than that of the BEST$^+$ radicals in all cases (Figure 12), confirming the absence of a significant magnetic contribution from the organic sublattice, as observed in the SQUID susceptibility measurements.

Conclusions. In this work we have shown the possibility of combining the seleniated donor molecule BEST with the octahedral anions [M(C$_2$O$_4$)$_3$]$^{3-}$ (M^{III} = Fe, Cr). Five novel radical salts have been obtained, namely (BEST)$_4$[M(C$_2$O$_4$)$_3$]·PhCOOH·H$_2$O with M^{III} = Cr (**1**) or Fe (**2**), (BEST)$_4$[M(C$_2$O$_4$)$_3$]·1.5H$_2$O with M^{III} = Cr (**3**) or Fe (**4**), and (BEST)$_9$[Fe(C$_2$O$_4$)$_3$]$_2$·7H$_2$O (**5**). Despite the tendency of the tris(oxalato)metalate anions to form pseudohexagonal anionic layers (as is the case in the radical salts of the ET donor), the anionic layers present in the BEST salts are very different. In **1** and **2** the pseudohexagonal lattice is disrupted by the inclusion of PhCOOH molecules in the layer which form H-bonds to the oxygen atoms of the anions. In compounds **3**−**5** the anions are too separated (in average) and cannot give rise to a pseudohexagonal arrangement. In all the salts the organic layers exhibit the same typical β-type phase, although they are formed by different types of BEST stackings: in **1** and **2** the BEST molecules stack forming

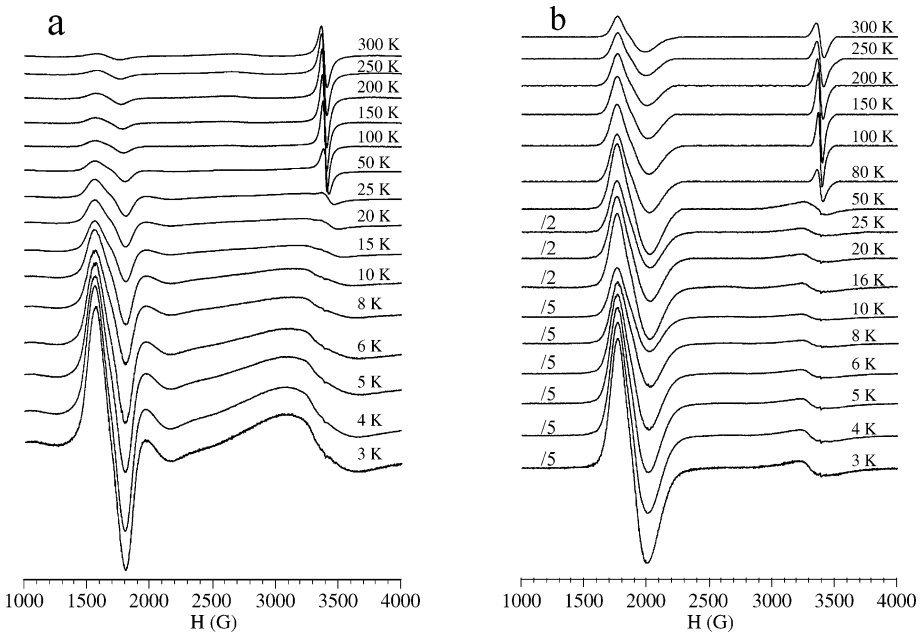

Figure 12. X-band ESR spectrum at different temperatures of an Fe-containing salt, $(BEST)_4[Fe(C_2O_4)_3]\cdot PhCOOH\cdot H_2O$ (**2**) (a), and a Cr-containing one, $(BEST)_4[Cr(C_2O_4)_3]\cdot 1.5H_2O$ (**3**) (b).

tetramers (β_{82}), in **3** they form dimers ($\beta_{21\times2}$), and in **5** they form trimers ($\beta_{31\times3}$). All compounds are paramagnetic semiconductors in which the magnetic susceptibility is dominated by the Fe- or Cr-containing anions. All the salts exhibit high room-temperature conductivities due to the presence of short chalcogen···chalcogen contacts, while the existence of some fully ionized donor molecules in all the salts accounts for the observed semiconducting behaviors. The magnetic properties have shown the presence of high-spin isolated Fe^{III} and Cr^{III} anions and no noticeable contribution form the organic sublattice, as confirmed by the ESR spectra that show a weak and narrow signal coming from some isolated $BEST^+$ radicals ($g_{BEST} = 2.004-2.006$, with $\Delta H = 55-35$ G) and the much more intense signals from the anions, with a perpendicular component at 1600−1800 G ($g_\perp = 3.60-4.48$, with $\Delta H = 180-230$ G) and a parallel one at ca. 3300 G ($g_{||} = 2.04-2.05$ with $\Delta H = 220-460$ G).

Acknowledgment. We thank the Spanish Ministerio de Educación y Ciencia (MEC) (Project CTQ2005-09385-C03-01/PPQ), and the European Union (COST Action D35/0011/05) for financial support. C.G.-S. thanks the MEC for a "Ramón y Cajal" research contract. S.C. thanks the MEC for a predoctoral grant. A.A. thanks Homerton College for a Junior Research Fellowship.

Supporting Information Available: Crystallographic data for compounds **1**−**3** and **5** in CIF format and tables listing intermolecular S···S, S···Se, and Se···Se distances for **1**−**3** and **5**. This material is available free of charge via the Internet at http://pubs.acs.org.

IC061494P